Macromolecules
ARTICLE

Macromolecules **2010**, *43*, 6343–6347 **6343**
DOI: 10.1021/ma1010759

Organosilica Nanoshells with Thin Silica Cross-Linking by Miniemulsion Periphery Polymerization (MEPP)

Ronan McHale,[†] Negar Ghasdian,[†] Nicole S. Hondow,[‡] Peter M. Richardson,[§] Alison M. Voice,[§] Rik Brydson,[‡] and Xiaosong Wang*[,†]

[†]*Department of Colour Science, School of Chemistry,* [‡]*Institute for Materials Research* (*SPEME*), *and* [§]*Polymer IRC, School of Physics and Astronomy, University of Leeds, Leeds LS2 9JT, U.K.*

Received March 15, 2010; Revised Manuscript Received June 17, 2010

ABSTRACT: Organosilica nanoshells with a thin silica cross-link and large internal cavity have been prepared via the miniemulsion periphery polymerization (MEPP) process. Triethoxysilyl-terminated triblock copolymer surfactants were used to stabilize an oil-in-water miniemulsion. Subsequent cross-linking of the terminal silyl functionality yielded hybrid (organosilica) hollow nanoshells. The unique structural design of the shells (large internal cavity and thin porous cross-link) ensured an interesting combination of properties, including high thermal stability, high efficiency of encapsulation, and trans-shell diffusion of ions.

Introduction

Miniemulsion periphery polymerization (MEPP) is a recently reported technique from our group allowing for the synthesis of well-defined, uniform hollow nanoshells in a facile one-pot synthesis. Miniemulsions comprise a surfactant-stabilized dispersion of oil droplets in a continuous water phase (or vice versa). The MEPP process involves the confinement of cross-linkable species at the periphery of such oil droplets using terminally functionalized polymeric surfactants. Subsequent cross-linking yields nanoshells with large internal cavities capable of efficient encapsulation. Given the diverse range of functionalities available in the molecular toolbox, it is envisaged that a wide variety of both inorganic and organic nanoshells are accessible via the MEPP process. To date, pentacyanoferrate-terminated surfactants have been used as the miniemulsion stabilizers which, on cross-linking in the presence of Fe^{3+}, yield Prussian Blue (PB) metal coordination polymer nanoshells with variable sizes and morphologies.[1−3]

Silica-containing nanoparticles have of late been subjected to rigorous investigation[4−14] owing to their many potential applications as vectors in targeted drug dispensing and bioimaging.[15−17] Research in this area has gained further impetus due to the biocompatibility, high stability, low toxicity, and optical transparency of silica. A number of supramolecular templating approaches have been used to synthesize both hollow and core−shell organosilica nanoparticles with varying silica contents. One such approach involves the covalent incorporation of silyl functionality into the backbone or termini of micellar building blocks which duly cross-link under appropriate conditions to achieve micellar stabilization.[4−7] Du et al., for example, self-assembled poly(ethylene oxide)-*block*-poly(3-(trimethoxysilyl)propyl methacrylate) (PEO-*b*-PTMSPMA) in MeOH/water mixtures to yield, on cross-linking, organic/inorganic hybrid vesicles with silica walls.[5] Another approach involves interfacial deposition of low molecular weight silica precursors (e.g., tetraethoxysilane; TEOS) onto preformed polymeric micellar templates.[8,9,11,13,17−19] A common feature of all these micellar systems is the presence of multiple layers of silica cross-linking. While such a design component is often desirable in the pursuit of improved micellar stabilization and/or lower porosity in the vesicle wall, it can also, depending on the application, offer constraints such as limited encapsulation efficiency, lower internal encapsulation volume, less flexibility in swelling/deswelling, and slow diffusion of guest materials, etc.

Herein, we illustrate the versatility of the MEPP process by extending its chemistry to silyl-terminated surfactants, thereby generating novel thin organosilica nanoshells with a large internal cavity (see Scheme 1). The cross-linked nanoshells enable robust and stable encapsulation as well as high thermal resistance and also possess an efficient trans-shell transport capability.

Experimental Section

Materials. Poly(ethylene glycol)-*b*-poly(propylene glycol)-*b*-poly(ethylene glycol) ($PEO_{122}PPO_{56}PEO_{122}$; EPE-OH) triblock copolymer ($M_n \sim 14\,000$ g/mol), 3-(triethoxysilyl)propyl isocyanate, triethylamine (TEA), and $FeCl_2.4H_2O$ were purchased from Sigma-Aldrich (United Kingdom) and used without further purification, unless otherwise indicated. Toluene (anhydrous; Sigma-Aldrich), tetrahydrofuran (THF; anhydrous; Sigma Aldrich), methanol (MeOH; reagent grade; Fisher Scientific), diethyl ether (Et_2O; reagent grade; Sigma-Aldrich), and hexadecane (HD; Alfa Aesar) were used without further purification. 2-Butyl-6-(butylamino)-1*H*-benzo[*de*]isoquinoline-1,3(2*H*)-dione fluorescent dye was kindly synthesized and supplied by Prof. John Griffiths and Dr. John Mama (School of Chemistry, University of Leeds). It is also available under the commercial name Fluorol 555 (Exciton).

Characterization. A transmission electron microscope (TEM; Philips CM-10) with an acceleration voltage of 80 kV was used to take low-resolution TEM images. A field emission gun TEM microscope (Philips CM200 FEGTEM; 200 kV) equipped with a Gatan GIF200 imaging filter running DigitalMicrograph software was used to take higher resolution TEM images and perform elemental mapping. TEM samples were prepared by placing a drop of diluted miniemulsion (1 part miniemulsion to 4 parts water) onto a carbon-coated copper grid, letting rest for ~30 s, quickly removing excess miniemulsion using filter paper, and drying under ambient conditions. The specimens were stained by dipping the dried TEM grids into a sodium phosphate buffered solution of OsO_4 (0.25 g OsO_4 in 25 mL of 0.1 M buffer) followed by quick removal of excess stain.

SEM micrographs were obtained using a LEO 1530 Gemini FEGSEM (3 kV). SEM samples were prepared by letting a drop

*Corresponding author: Fax 0044-113-3432947; e-mail X.S.Wang@leeds.ac.uk.

Published on Web 07/08/2010

Scheme 1. Synthesis of Organosilica Nanoshells with Thin Silica Cross-Link by Miniemulsion Periphery Polymerization (MEPP) (above) and Color Coordinated Structure of EPE-Si Surfactant (below)[a]

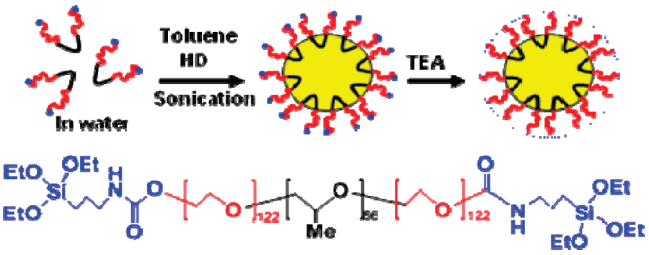

[a] HD = hexadecane, TEA = triethylamine.

of miniemulsion dry on an aluminum SEM stub. SEM specimens were coated with a gold/platinum alloy thin film prior to observation.

Confocal microscopy images were acquired on a Zeiss LSM510 META confocal microscope using a 63× oil immersion lens. Particles were imaged using 458 nm laser excitation light. Emission signals above 505 nm were collected with a 505LP long pass emission filter. A digital zoom factor of 7 was used with images measuring 512 pixels square. Images were imported into ImageJ for analysis. 3D plots were generated with Surface Plot.

TGA curves were recorded using a TA Instruments (TGA-2900 model) thermobalance in a temperature range of 25−550 °C at a heating rate of 10 °C/min under N_2. Fluorescence measurements were recorded at room temperature on a Jobin Yvon-SPEX FluoroMax-3 fluorimeter with excitation wavelength set at 432 nm and 0.1 s of integration time. The slits for both excitation and emission were set at 1.5 nm. IR spectra were recorded using a Perkin-Elmer 2000 FT-IR spectrophotometer. Dry samples were used directly without any sample preparation using the Golden Gate Diamond ATR mode of the FT-IR machine. Dynamic light scattering (DLS) hydrodynamic diameter data were recorded at $\theta = 90°$ on a Brookhaven Instruments system (Ser. No.: BI-APD) equipped with a Melles Griot HeNe laser ($\lambda = 632.8$ nm). Zeta potential data were acquired on a Malvern Zetasizer Nano-ZS system. NMR spectra were recorded on a Bruker 500 MHz Ultrashield system.

Synthesis of Triethoxysilyl-Terminated Poly(ethylene glycol)-*b*-poly(propylene glycol)-*b*-poly(ethylene glycol) Triblock Copolymer (EPE-Si). Poly(ethylene glycol)-*b*-poly(propylene glycol)-*b*-poly(ethylene glycol) triblock copolymers (7.5 g), were dried using azeotropic distillation at 110 °C under N_2 from their anhydrous toluene solution (∼100 mL). Anhydrous THF (20 mL) was then added at room temperature while maintaining a N_2 atmosphere. Subsequently, 1.5 g (6 mmol) of 3-(triethoxysilyl)propyl isocyanate and 0.61 g (6 mmol) of TEA were added to the prepared solution. Afterward, the reaction mixture was stirred under reflux at 65 °C for 3 days, with a N_2 atmosphere maintained throughout. On cooling, ∼90% of the solvent was removed under vacuum. The resultant concentrated mixture was then precipitated into ∼300 mL of cold Et_2O. The precipitated polymer was collected by filtration and further purified by 3 or 4 cycles of dissolving in a small amount of DCM (∼15 mL) and precipitation into cold Et_2O, followed by a final filtration and drying overnight under vacuum at ambient temperature. Triethoxysilyl functionality was calculated to be >95% by comparison of the $-CH_2-O-(C=O)-NH-$ ^1H NMR peak at 4.18 ppm with the $OCH_2CH(CH_3)$ peak at 1.16 ppm. ^1H NMR (MeOD, 500 MHz): 4.18 (m, 4H, $-CH_2-O-(C=O)-NH-$), 3.85 (q, 12H, $-Si-O-CH_2-CH_3$), 3.66 (m, 972H, OCH_2CH_2O), 3.55 (m, 112H, $OCH_2CH(CH_3)$), 3.49 (m, 56H, $OCH_2CH(CH_3)$), 3.10 (t, 4H, $-NH-CH_2-CH_2-$), 1.60 (m, 4H, $-CH_2-CH_2-CH_2-$), 1.24 (t, 18H, $-Si-O-CH_2-CH_3$) 1.16 (m, 168H, $OCH_2CH(CH_3)$), 0.63 (t, 4H, $-CH_2-Si-$).

Preparation of Organosilica Nanoshells. To prepare the nanoshells, toluene (0.5 g) was first mixed with hexadecane (HD) (20 mg). This organic phase was then added to the aqueous

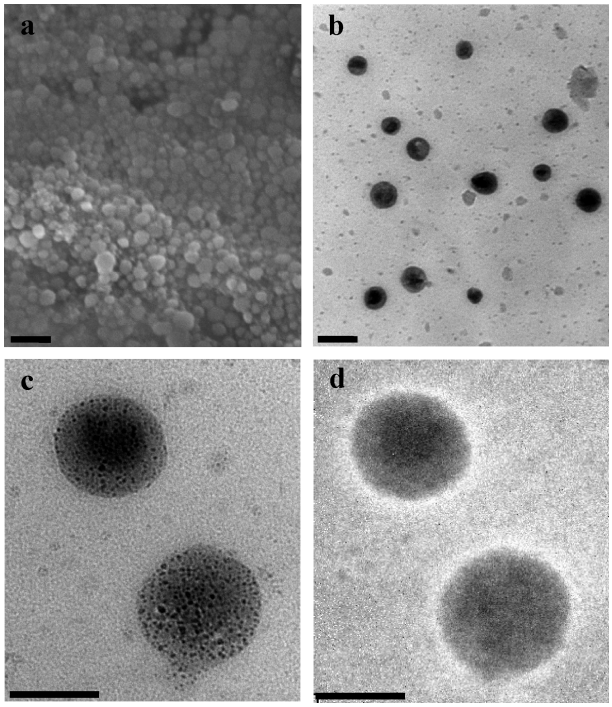

Figure 1. (a) SEM image of organosilica nanoshells (scale bar = 200 nm). (b) TEM image of OsO_4 stained organosilica nanoshells with naphthalimide dye encapsulated. Note the selective staining of the hollow dye containing centers due to affinity of OsO_4 for unsaturation in the dye (scale bar = 200 nm). (c) Higher magnification TEM images of nanoshells similar to those in (b) (scale bar = 100 nm). (d) EFTEM carbon K-edge elemental mapping of the organosilica nanoshells shown in (c). Lighter colored regions in the EFTEM image denote highest concentrations of carbon (scale bar = 100 nm).

phase consisting of distilled water (9.08 g) and 0.4 g of EPE-Si under vigorous stirring. After 45 min, the mixture was sonicated (Bandelin Sonopuls HD2200, 60% power) for a period of 15 min. The resultant miniemulsion was stable for a period of months. To prepare the nanoshells, ∼30 mg of TEA was added to the above miniemulsion to induce cross-linking via hydrolysis and condensation reactions. For TEM imaging and confocal microscopy, 2.5 mg of 2-butyl-6-butylaminobenzo[*de*]isoquinoline-1,3-dione was dissolved in the toluene (0.5 g) prior to mixing of the oil and water phases. For fluorescence quenching studies, a lower concentration of the dye was used (0.025 mg in 0.5 g of toluene).

Results and Discussion

As the first step in synthesizing organosilica nanoshells with a thin silica cross-link, triethoxysilyl-terminated poly(ethylene glycol)-*b*-poly(propylene oxide)-*b*-poly(ethylene oxide) (EPE-Si) was prepared (see Experimental Section). This functionalized surfactant was then employed in the MEPP process as illustrated in Scheme 1.

In a typical experiment, miniemulsions were prepared from a mixture of water, EPE-Si, toluene, and hexadecane (90.8:4:5:0.2 w/w). Triethylamine (TEA) was added to the miniemulsions to aid cross-linking of the triethoxysilyl functionality. On stirring, the miniemulsion became progressively cloudier, thus representing the first indication of silica formation at the periphery. Miniemulsions were colloidally stable over a period of months, indicating that cross-linking had no adverse effect on stability.

The morphology of the product obtained from the MEPP process outlined in Scheme 1 was initially assessed using scanning electron microscopy (SEM). As shown in Figure 1a, the product consisted of spherical nanoparticles approximately 80−100 nm in

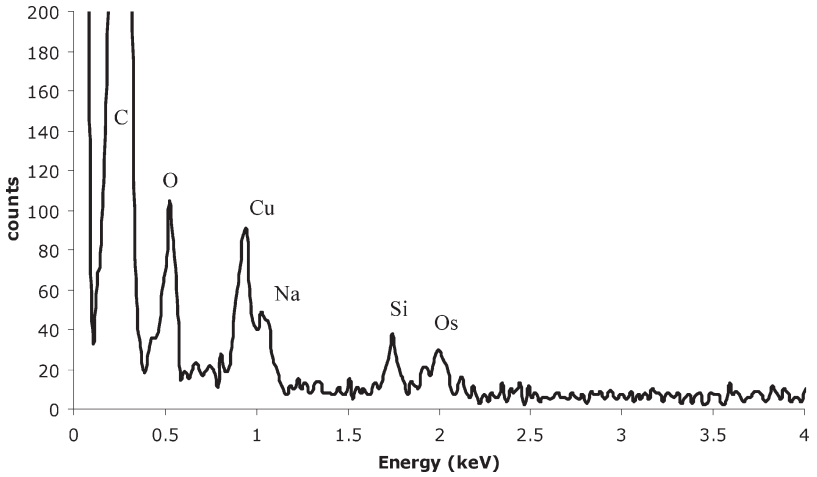

Figure 2. EDX spectrum of OsO_4 stained organosilica nanoshells showing C, O, and Si peaks of the nanoshells, Os peak from the staining agent, and Cu peak of the TEM grids. The Na peak is due to the buffer solution used to prepare the OsO_4 stain.

diameter. The observation of large populations of nanospheres in the dry state provides strong preliminary evidence that sufficient silica cross-linking occurred at the periphery of the droplets to retain nanostructure on drying.

The hollow nature of the shells was investigated using transmission electron microscopy (TEM). To aid TEM imaging of the nanoshells, a hydrophobic naphthalimide fluorescent dye was encapsulated by addition to the toluene phase prior to miniemulsion formation. Fluorescence confocal microscopy of the dye-containing nanoshells in solution was also conducted. As is evident in Figure S1, individual nanoshells are clearly identifiable as bright spots (inset) and peaks (main image), thus indicating the dye is encapsulated within the nanoshells. The encapsulated dye allows the cavity of the shell to be probed using OsO_4 as a staining agent in TEM analysis. OsO_4 selectively stains dye containing regions due to the affinity of OsO_4 for unsaturation in the dye, thus affording clearer characterization of the hollow nature of the nanoshells. As can be clearly seen in Figure 1b,c, the cores of the nanoshells exhibit the highest electron density; i.e., they have been selectively stained by OsO_4. This observation confirms that the shells possess a significantly large cavity as well as considerable encapsulation and retention capabilities. The absence of highly electron dense regions exterior to the nanoshells suggests dye encapsulation is close to quantitative.

Energy filtered TEM (EFTEM) enabled carbon elemental mapping of individual nanoshells to further probe their chemical makeup. As seen in Figure 1d, the highest concentration of carbon (bright rings) was seen at the periphery of the nanoshells, as expected. The carbon halos are not visible in the original TEM image (Figure 1c) as this region contains no unsaturated functionality and thus was not stained by OsO_4. Elemental mapping for Si was also attempted. However, despite detecting the presence of Si by EDX (Figure 2), the very low concentration of this element in the nanoshells precluded the assignment of a reliable electron energy-loss (EELS) peak, thus preventing the construction of an elemental map for Si. This is unsurprising, considering the thin nature of the silica shell and the fact that the Os $O_{2,3}$-edge will contribute to the background before the Si $L_{2,3}$-edge. Overall, EFTEM analysis further confirms the hollow nature of the nanoshells and the presence of a thin organosilica wall, in agreement with the MEPP formation mechanism.

As a fundamental test for nanoshell formation, i.e., to confirm a degree of cross-linking occurred sufficient to retain structure of the nanoshells in the absence of a templating oil phase, the miniemulsions were diluted in methanol until they became clear. Significantly, nanoshell structure was retained, as evidenced by

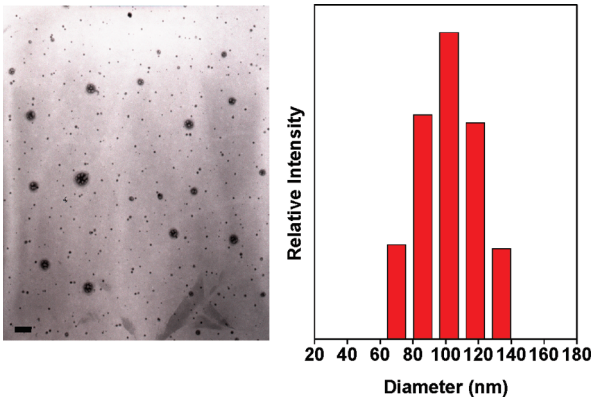

Figure 3. TEM image of methanol diluted (1 part miniemulsion:5 parts MeOH) and OsO_4 stained organosilica nanoshells containing naphthalimide dye (scale bar = 200 nm) and the corresponding dynamic light scattering (DLS) data of the same methanol diluted miniemulsion.

the observation of nanoshells by TEM (see Figure 3) of similar size to those in Figure 1. The appearance of small (~10−15 nm) nanoparticles exterior to the nanoshells in Figure 3 suggests that a quantity of the dye cargo was lost on mixing of the oil and water phases. A highly porous thin shell structure can account for this releasing behavior. Dynamic light scattering (DLS) analysis of the methanol diluted miniemulsions also supported retention of the nanoshell structure, as evidenced by a DLS distribution centered at ~100 nm (Figure 3). (*Note*: The DLS data shown in Figure 3 were taken immediately on addition of methanol to the cross-linked miniemulsion. A peak at ~10 μm was also present (see Figure S2) presumably due to the poor solubility and thus agglomeration and precipitation of the cross-linked nanoshells from the methanol/miniemulsion solution. On leaving the solution to rest, the appearance of visible precipitates confirmed poor solubility. Subsequent DLS analysis revealed the peak at 100 nm to disappear due to complete precipitation of the nanoshells.) A control DLS experiment on a methanol diluted miniemulsion stabilized by nonfunctionalized EPE (EPE−OH) gave no light scattering response. TEM analysis of the same EPE-OH stabilized miniemulsion also revealed an absence of spherical and/or hollow nanostructures.

To acquire further evidence for the formation of Si−O−Si cross-linking, a number of chemical analyses were conducted. FT-IR spectroscopy revealed the presence of a band at 717 cm^{-1} in the organosilica nanoshells which was absent in both the

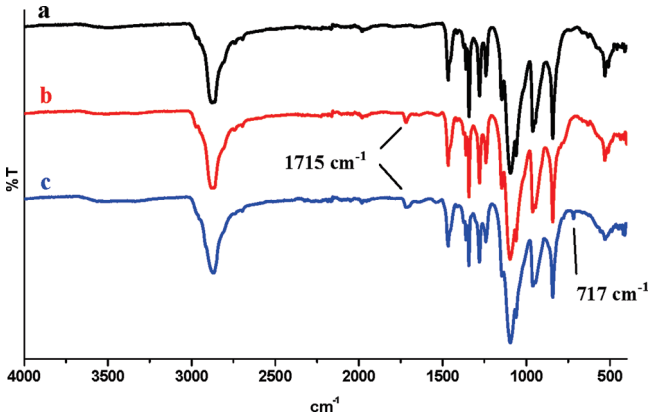

Figure 4. FT-IR spectra of EPE-OH (a), EPE-Si (b), and organosilica nanoshells (c). The new band at 717 cm^{-1} in the organosilica nanoshells corresponds to the symmetric stretch of Si−O−Si. The new band at 1715 cm^{-1} in (b) and (c) corresponds to the urethane linker of the triethoxysilyl end group in EPE-Si.

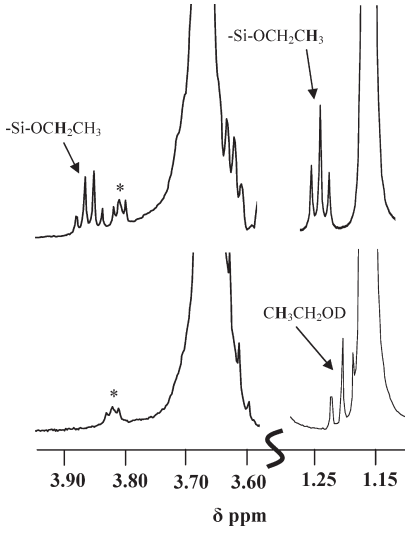

Figure 5. ^{1}H NMR spectra (MeOD) of EPE-Si (top) and the EPE-Si stabilized miniemulsion after stirring in the presence of TEA (bottom). The miniemulsion was prepared using D_2O (to reduce the water peak) before dilution in MeOD for analysis. See Experimental Section for assignments of polymeric (large) resonances. Peak marked with an asterisk was present in original EPE-OH surfactant. Curved line on the scale bar between 3.60 and 1.25 denotes a break in the spectrum at this point.

nonfunctionalized starting material (EPE-OH) and EPE-Si (Figure 4). This band has previously been assigned as the symmetric stretch of Si−O−Si.[20−22] On magnification of the spectrum (Figure S3) a new peak was observed between 400 and 450 cm^{-1}, indicative of an Si−O−Si bending mode.[17,21,22] Si−O−Si antisymmetric stretching (∼ 1100 cm^{-1}) is likely swamped by the larger EPE absorbances.[17] The absence of a peak for Si−OH hydrogen bonded to water at ∼3289 cm^{-1}[23] suggests the vast majority of silanol (Si−OH) groups condensed into Si−O−Si linkages. Zeta potential analysis revealed little charge on the surface of the nanoshells after cross-linking (−3.38 mV). This finding also supports the absence of significant numbers of silanol groups at the periphery of the nanoshells.

^{1}H NMR spectroscopy revealed quantitative hydrolysis of triethoxysilyl end groups to silanols as evidenced by the disappearance of the triplet and quartet assigned to the ethoxysilyl resonance at 1.24 and 3.85 ppm, respectively (see Figure 5, top) and the appearance of the characteristic triplet of ethanol, the hydrolysis product, at 1.19 ppm (peak slightly hidden; Figure 5, bottom). (*Note*: The ethanol product should be of the form CH_3CH_2OD due to the presence of D_2O.) The quartet for ethanol (expected at ∼3.60−3.65 ppm) is presumed hidden by the large polymer resonance in this region. ^{29}Si NMR analyses of both the nondiluted D_2O miniemulsion and the MeOD diluted miniemulsion were also attempted. However, despite using 10 mm PTFE NMR tubes and 2000 scans, no appreciable silica signal was observed. This is understandable considering the low percentage of Si atoms in the nanoshells (2 Si atoms per polymer chain (M_n ∼ 14 000 g/mol) together with the low isotopic abundance of ^{29}Si and long relaxation times.

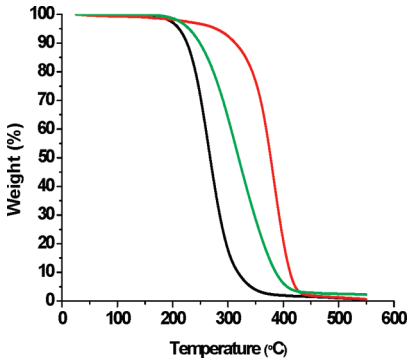

Figure 6. Thermogravimetric analysis of EPE-OH (black line), EPE-Si (green), and organosilica nanoshells (red).

To the best of our knowledge, this work embodies the first report of well-characterized, thin organosilica nanoshells possessing a large internal cavity capable of quantitative encapsulation. The protocol described herein has numerous advantages over that used to generate siloxane nanocages by cross-linking micellar triethoxysilyl(propylcetylcarbamate) surfactants[7] and other micellar systems with multiple layers of silica cross-linking.[4−6,8,9,11,13,17] Triethoxysilyl(propylcetylcarbamate) micellar systems are inherently less well-defined compared to miniemulsions due to a dynamic equilibrium between unimers and micelles in solution and a high cmc. Such systems also result in comparatively small products (2−5 nm),[7] making direct characterization of internal cavities and/or encapsulation difficult. The core−shell nature of micelles often necessitates the removal of hydrophobic cores post-cross-linking to generate encapsulation capabilities.[7] Further, encapsulation in micellar systems normally relies on diffusion and sequestration from solution and thus is comparatively inefficient compared to the MEPP system herein, whereby encapsulated materials reside within the oil droplets prior to cross-linking. As alluded to in the introduction, the vast majority of silica-containing nanoshells reported to date possess numerous layers of silica cross-linking which often blocks the transport of materials across the shell membrane. Considering the large internal void capacity and thin nature of the nanoshells described herein, numerous properties such as thermal stability and facile trans-shell transport can be expected.

Thermogravimetric analysis (TGA) was conducted on EPE-OH, EPE-Si, and the dry organosilica nanoshells (Figure 6). The nanoshells exhibited a resistance to heat significantly greater than that of EPE-OH, with a difference of ∼100 °C observed in the temperature at which maximum weight loss occurred. Compared with EPE-Si, the nanoshells also showed obviously higher thermal stability. This improved stability can be rationalized by the presence of extensive cross-linking in the nanoshells as well as a possible heat insulation contribution due to the internal cavities.[1]

Nanoshells with a thin silica cross-link should facilitate transport of guest materials. This property was probed by fluorescent quenching measurements. It is well-known that Fe^{2+} ions quench naphthalimide type dyes by a heavy atom effect.[24] Fluorescent intensity measurements (Figure 7) were taken from miniemulsions

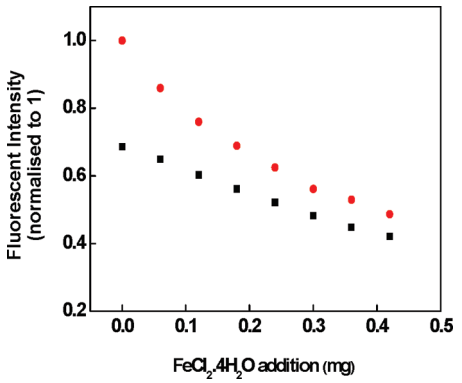

Figure 7. Fluorescence intensity measurements of naphthalimide dye containing cross-linked organosilica nanoshells (●) and non-cross-linked (■) miniemulsion droplets (containing the same concentration of dye) versus increasing levels of addition of $FeCl_2 \cdot 4H_2O$ as quencher. Measurements were taken immediately (after shaking) on addition of Fe^{2+} stock solution (3 mg $FeCl_2 \cdot 4H_2O$/mL H_2O) in 20 μL aliquots to 3 mL diluted miniemulsion sample for each data point. Note: miniemulsion samples were diluted (1 part miniemulsion to 4 parts H_2O) prior to analysis (see text for discussion).

containing a hydrophobic organosoluble dye (both cross-linked and non-cross-linked (EPE-OH stabilized) miniemulsions). Prior to the analysis, the miniemulsions were diluted (1 part miniemulsion:4 parts water). On dilution, the fluorescence of the non-cross-linked control dropped to a greater extent than the cross-linked nanoshells (from $\sim 2.2 \times 10^6$ cps in each case); hence, the quenching experiments started from different fluorescence intensities (see Figure 7). This preliminary observation indicates significant loss of dye from the non-cross-linked control on dilution and thus a more robust and stable encapsulation ability in the cross-linked nanoshells. (*Note*: Fluorescence of the dye in the water phase is negligible.) On addition of increasing levels of Fe^{2+}, the fluorescent intensities of both the cross-linked nanoshells and non-cross-linked control converged from their disparate starting points, with a slightly higher level of fluorescence retained in the cross-linked sample. One can conclude that the cross-linked organosilica nanoshells are more robust and stable to dilution than their non-cross-linked counterparts; however, ion diffusion through the nanoshells is not significantly altered on cross-linking. These findings underline a fundamental property of the nanoshells presented in this article; structural integrity of nanocapsules can be achieved without unduly effecting trans-shell transport. This combination of properties points at a potential application of this material as building blocks for high ion conductivity nanoelectrolytes. A brief investigation of such a possibility is detailed in the Supporting Information.

Conclusions

Novel organosilica nanoshells have been prepared from triethoxysilyl-terminated poly(ethylene glycol)-*b*-poly(propylene oxide)-*b*-poly(ethylene oxide) (EPE-Si) via the recently developed miniemulsion periphery polymerization (MEPP) technique. The obtained nanoshells were fully characterized as containing large internal cavities formed by thin silica cross-linking of the silyl-functionalized EPE surfactant. These unique structural features improve the thermal stability of the nanoshells in the dry state and render the nanoshells efficient in ion diffusion across the shell when in solution. A potential application as a high ion conductivity nanoelectrolyte is proposed.

Acknowledgment. This work was financially supported by The Engineering and Physical Sciences Research Council, UK (EPSRC). X.W. thanks EPSRC for an award of a Roberts Fellowship, and R.M. thanks EPSRC for a PDRA fellowship. We acknowledge Dr. Gareth Howell (University of Leeds) for confocal microscopy studies and Prof. John Griffiths and Dr. John Mama (both University of Leeds) for provision of the dye.

Supporting Information Available: Confocal microscopy image, supplemental DLS, FT-IR, and SEM data, and details of electroanalytical investigations into potential application of the nanoshells as high ion conductivity nanoelectrolytes. This material is available free of charge via the Internet at http://pubs.acs.org.

References and Notes

(1) Liang, G.; Xu, J.; Wang, X. *J. Am. Chem. Soc.* **2009**, *131*, 5378–5379.
(2) McHale, R.; Ghasdian, N.; Liu, Y.; Ward, M.; Hondow, N. S.; Brydson, R.; Wang, X. *Chem. Commun.* **2010**, *46*, 4574–4576.
(3) Wang, X.; McHale, R. *Macromol. Rapid Commun.* **2010**, *31*, 331–350.
(4) Koh, K.; Ohno, K.; Tsujii, Y.; Fukuda, T. *Angew. Chem., Int. Ed.* **2003**, *42*, 4194–4197.
(5) Du, J.; Chen, Y.; Zhang, Y.; Han, C. C.; Fischer, K.; Schmidt, M. *J. Am. Chem. Soc.* **2003**, *125*, 14710–14711.
(6) Du, J.; Armes, S. P. *J. Am. Chem. Soc.* **2005**, *127*, 12800–12801.
(7) Suh, Y.-W.; Kung, M. C.; Wang, Y.; Kung, H. H. *J. Am. Chem. Soc.* **2006**, *128*, 2776–2777.
(8) Huo, Q.; Liu, J.; Wang, L.-Q.; Jiang, Y.; Lambert, T. N.; Fang, E. *J. Am. Chem. Soc.* **2006**, *128*, 6447–6453.
(9) Wang, H.; Wang, Y.; Zhou, X.; Zhou, L.; Tang, J.; Lei, J.; Yu, C. *Adv. Funct. Mater.* **2007**, *17*, 613–617.
(10) Wang, Q.; Liu, Y.; Yan, H. *Chem. Commun.* **2007**, 2339–2341.
(11) Khanal, A.; Inoue, Y.; Yada, M.; Nakashima, K. *J. Am. Chem. Soc.* **2007**, *129*, 1534–1535.
(12) Peng, B.; Chen, M.; Zhou, S.; Wu, L.; Ma, X. *J. Colloid Interface Sci.* **2008**, *321*, 67–73.
(13) Du, L.; Liao, S.; Khatib, H. A.; Stoddart, J. F.; Zink, J. I. *J. Am. Chem. Soc.* **2009**, *131*, 15136–15142.
(14) Guerrero-Martínez, A.; Pérez-Juste, J.; Liz-Marzán, L. M. *Adv. Mater.* **2010**, *22*, 1182–1195.
(15) Kim, J.; Kim, H. S.; Lee, L.; Kim, T.; Kim, H.; Yu, T.; Song, I. C.; Moon, W. K.; Hyeon, T. *Angew. Chem., Int. Ed.* **2008**, *47*, 8438–8441.
(16) Park, J.-H.; Gu, L.; von Maltzahn, G.; Ruoslahti, E.; Bhatia, S. N.; Sailor, M. J. *Nat. Mater.* **2009**, *8*, 331–336.
(17) Tan, H.; Liu, N. S.; He, B.; Wong, S. Y.; Chen, Z.-K.; Li, X.; Wang, J. *Chem. Commun.* **2009**, 6240–6242.
(18) Wang, H.; Patil, A. J.; Liu, K.; Petrov, S.; Mann, S.; Winnik, M. A.; Manners, I. *Adv. Mater.* **2009**, *21*, 1805–1808.
(19) Yuan, J.-J.; Mykhaylyk, O. O.; Ryan, A. J.; Armes, S. P. *J. Am. Chem. Soc.* **2007**, *129*, 1717–1723.
(20) Machida, K.-i.; Adachi, G.-y.; Shiokawa, J. *Bull. Chem. Soc. Jpn.* **1982**, *55*, 2854–2857.
(21) Li, L.; Li, G.; Smith, R. L.; Inomata, H. *Chem. Mater.* **2000**, *12*, 3705–3714.
(22) Ma, D.; Li, M.; Patil, A. J.; Mann, S. *Adv. Mater.* **2004**, *16*, 1838–1841.
(23) Zhou, Q.; Zhang, J.; Ren, Z.; Yan, S.; Xie, P.; Zhang, R. *Macromol. Rapid Commun.* **2008**, *29*, 1259–1263.
(24) Grabchev, I.; Chovelon, J.-M.; Bojinov, V. *Polym. Adv. Technol.* **2004**, *15*, 382–386.